

Fate of Antimony and Arsenic in Contaminated Waters at the Abandoned Su Suergiu Mine (Sardinia, Italy)

Rosa Cidu¹ · Elisabetta Dore¹ · Riccardo Biddau¹ · D. Kirk Nordstrom²

Received: 17 November 2016 / Accepted: 24 July 2017 / Published online: 31 July 2017
© Springer-Verlag GmbH Germany 2017

Abstract We investigated the fate of Sb and As downstream of the abandoned Su Suergiu mine (Sardinia, Italy) and surrounding areas. The mined area is a priority in the Sardinian remediation plan for contaminated sites due to the high concentrations of Sb and As in the mining-related wastes, which may impact the Flumendosa River that supplies water for agriculture and domestic uses. Hydrogeochemical surveys conducted from 2005 to 2015 produced time-series data and downstream profiles of water chemistry at 46 sites. Water was sampled at: springs and streams unaffected by mining; adits and streams in the mine area; drainage from the slag heaps; stream water downstream of the slag drainages; and the Flumendosa River downstream from the confluence of the contaminated waters. At specific sites, water sampling was repeated under different flow conditions, resulting in a total of 99 samples. The water samples were neutral to slightly alkaline. Elevated Sb (up to 30 mg L⁻¹) and As (up to 16 mg L⁻¹) concentrations were observed in water flowing from the slag materials from where the Sb ore was processed. These slag materials were the main Sb and As source at Su Suergiu. A strong base, Na-carbonate, from the foundry wastes, had a major influence on mobilizing Sb and As. Downstream contamination can be explained by considering that: (1) the predominant

aqueous species, Sb(OH)₆⁻ and HAsO₄⁻², are not favored in sorption processes at the observed pH conditions; (2) precipitation of Sb- and As-bearing solid phases was not observed, which is consistent with modeling results indicating undersaturation; and (3) the main decrease in dissolved Sb and As concentrations was by dilution. Dissolved As concentrations in the Flumendosa River did not generally exceed the EU limit of 10 µg L⁻¹, whereas dissolved Sb in the river downstream of the contamination source always exceeded the EU limit of 5 µg L⁻¹. Recent actions aimed at retaining runoff from the slag heaps are apparently not sufficiently mitigating contamination in the Flumendosa River.

Keywords Inorganic contaminants · Hydrogeochemistry · Slag materials · Mining environment

Introduction

Antimony (Sb) and arsenic (As) are potentially toxic contaminants, with tens to hundreds of thousands of individuals likely affected by mine waste-derived Sb (Kossoff et al. 2015), and millions of individuals affected by As toxicosis (Bhattacharya et al. 2007). Typical Sb concentrations in unpolluted waters are <1 µg L⁻¹, but concentrations can reach 100 times these levels in areas close to anthropogenic sources (Filella et al. 2002a). Sb is present in natural waters as both dissolved Sb(III), predominantly as Sb(OH)₃⁰, and dissolved Sb(V), predominantly as Sb(OH)₆⁻, the latter being considered less toxic (Filella et al. 2002b; Wilson et al. 2010). Typical concentrations of As in unpolluted waters are <10 µg L⁻¹ and frequently <1 µg L⁻¹ (Cidu et al. 2011; Reimann et al. 2009; Smedley and Kinniburgh 2002). Arsenic is mostly present in natural waters as dissolved

Electronic supplementary material The online version of this article (doi:10.1007/s10230-017-0479-8) contains supplementary material, which is available to authorized users.

✉ Rosa Cidu
cidur@unica.it

¹ Dipartimento di Scienze Chimiche e Geologiche, Cagliari University, via Trentino 51, 09127 Cagliari, Italy

² US Geological Survey, 3215 Marine St., Boulder, CO 80303, USA

As(III)-bearing species [As(OH)₃⁰] or dissolved As(V)-bearing species [AsO(OH)₃⁰] and dissociated species], with As(V) being considered less toxic (Mandal 2015). The World Health Organization (WHO 2011) has established guideline values of 20 µg L⁻¹ Sb and 10 µg L⁻¹ As for drinking water, while the European Community uses values of 5 µg L⁻¹ Sb and 10 µg L⁻¹ As (Council of the European Union 1998).

Particularly high concentrations of Sb (Casiot et al. 2007; Filella et al. 2009) and As (Asaoka et al. 2012; Craw et al. 2003; Frau et al. 2012; Ondrejková et al. 2013; Ritchie et al. 2013) may occur in water draining from abandoned mine sites. Several studies have investigated the similarities and differences of Sb and As in aquatic systems (Masson et al. 2009; Willis et al. 2011), including mining environments (Asaoka et al. 2012; Beauchemin et al. 2012; Carvalho et al. 2014; Casiot et al. 2007; Fawcett et al. 2015; Hiller et al. 2012; Mitsunobu et al. 2006; Okkenhaug et al. 2012; Ondrejková et al. 2013; Ritchie et al. 2013). Results indicate that different processes can affect the fate of aqueous Sb and As in mining environments. Like As, dissolved Sb can be sequestered by iron oxides (Wang et al. 2011) and/or precipitated in secondary Sb-bearing minerals (Roper et al. 2012), but can also persist in solution for tens of kilometers from the contamination source (Ashley et al. 2003; Cidu 2011). The geochemistry behind these differences in behavior are important to understand.

This study investigated the fate of Sb and As in drainage waters from the abandoned Sb Su Suergiu mine (Sardinia, Italy) and the receiving waters of the Flumendosa River. The area is heavily contaminated by Sb and As, with contaminated surface waters used for agricultural and domestic needs (Cidu et al. 2014 and references therein). The previous study (Cidu et al. 2014) reported on Sb only and its dispersion in soils, water, and vegetation. This study presents new data on dissolved As as well, compares the hydrochemistry of As and Sb in receiving waters including the main river system, and presents long-term time series trends in water chemistry (2005–2015). It also focuses more on the importance of the source waste and its contribution to Sb and As mobility. In 2008, the Sardinian Regional Government recognized Su Suergiu as a priority in the remediation plan for contaminated sites in Sardinia. Considering the scarcity of funds available for remediation, results from this study can provide valuable insight for further remediation and management. This study can also determine the likely degree of natural attenuation expected in this fluvial system. Results can be used to establish baseline conditions in Sb-As-contaminated areas in Sardinia and elsewhere, and the capacity for natural attenuation.

Study Area and Mining History

Location and Mine History

The study area is located in southeastern Sardinia (39°29'N; 09°39'E), in the Gerrei mining district, and includes the abandoned Su Suergiu mine, the Rio Ciurixeda catchment area and the lower part of the Flumendosa River (Fig. 1a). The area contains low-grade metamorphic rocks belonging to allocthonous units emplaced during the Hercynian orogenesis (Carmignani et al. 1986).

The mineralization at Su Suergiu was linked to magmatic-hydrothermal activity contemporaneous with the main Hercynian deformation phase (Funedda et al. 2005). It includes stibnite, scheelite, arsenopyrite, pyrite, and gold, with calcite and quartz in the gangue; mineralized lenses are arranged parallel to the foliation of highly deformed black shale and meta-limestone belonging to the cataclastic belt of the Villasalto Fault (Funedda et al. 2005). Underground mining took place from 1880 to 1960, with production peaks in the 1920–1930's. The foundry was active from 1882 to 1987, with Sb-ore coming from other Italian and foreign locations after the mine closed in 1960. The foundry products were about 7000 t of purified stibnite, 5000 t of Sb₂O₃, and 13,500 t of metallic Sb (Amat di San Filippo 2014). Materials used for Sb extraction included charcoal and Na-carbonate. Some of the residues from the foundry activity was reprocessed. After all mining activities ceased, mining-related wastes was either deposited on several heaps or strewn randomly on the ground (Fig. 1b). These wastes, consisting mainly of fine materials, are most often vegetated, while the wastes situated near streams show evidence of erosion. The foundry slag, consisting of residues from several periods of metallurgical processing, was dumped in two piles (about 66,000 m³; RAS 2003) in front of the foundry plant (Fig. 1b). They are devoid of vegetation and have been affected by significant erosion during storm runoff. At present, the only environmental mitigation consists of a retaining wall built on the edge of the slag heaps to divert runoff and minimize erosion. However, major storms have damaged the retaining wall and the foundry wastes have been transported by runoff for long distances downstream of the dump.

Site Characteristics

The climate is semi-humid, consisting of dry summers and variable rainfall, mostly occurring from October to April. Mean annual precipitation is 670 mm, and mean annual temperature is 16 °C (RAS 1998), based on local site data collected in 1955–1992. The permeability of the shale is 10⁻⁴–10⁻⁷ m s⁻¹; meta-limestones show higher

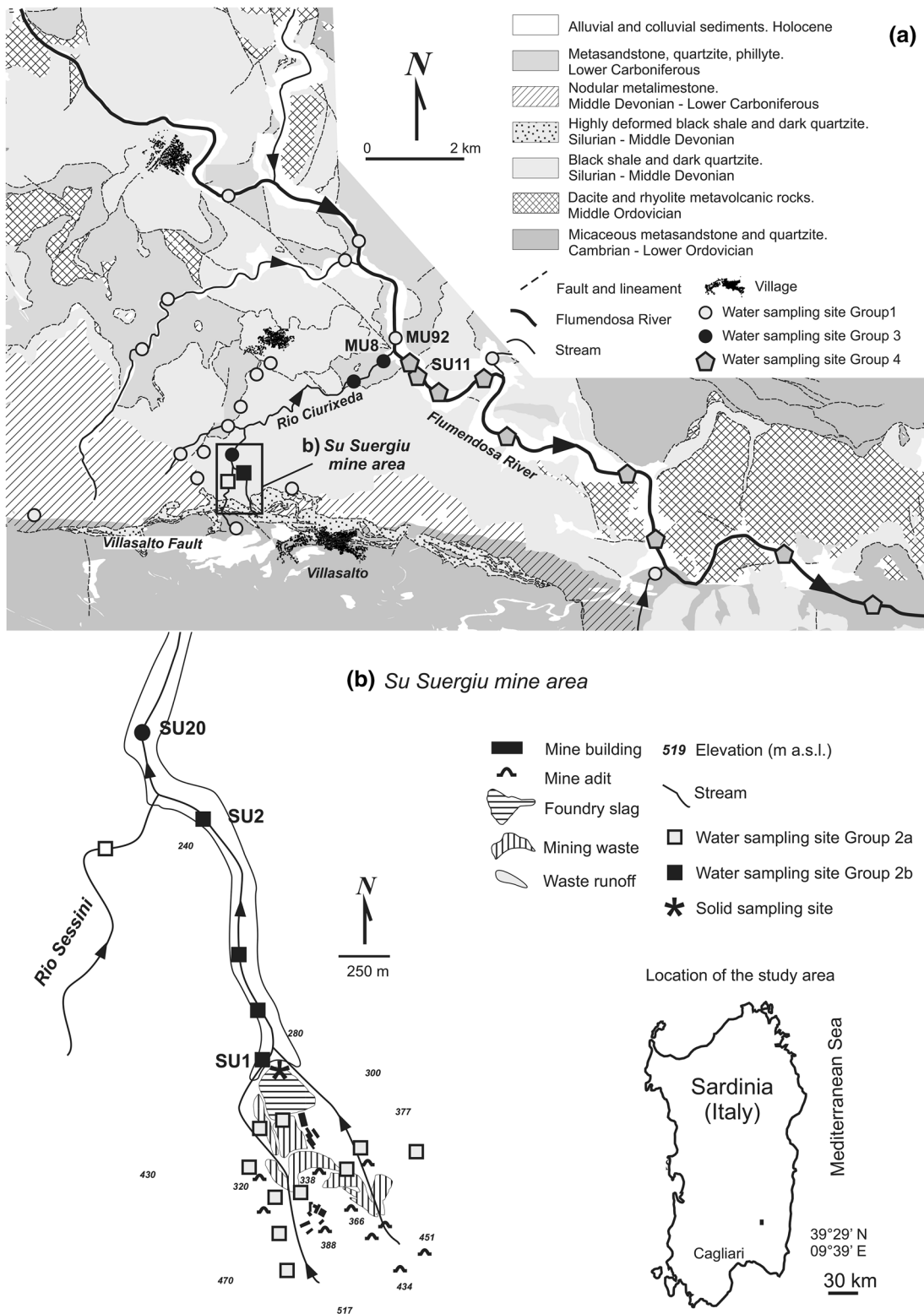


Fig. 1 Geological map of the Su Suergiu area (modified by RAS, 2013 and Cidu et al. 2014) showing the location of water and solid samples

permeability (10^{-2} – 10^{-4} m s⁻¹), but occur in very small outcrops (IGE 2009). Hence, springs are scarce, with low flows (<0.1 L s⁻¹ under high flow conditions) and represent groundwater circulation in the study area. The main water course of the area is the Flumendosa River (<300 L s⁻¹ and >1000 L s⁻¹, respectively, under low and high flow conditions). A few tributaries with perennial flow (>100 L s⁻¹ under high flow conditions) are present, whereas others are intermittent streams. Stream and river flow may vary substantially in a year because of the highly variable rainfall. The Rio Ciurixeda stream receives untreated drainage from the Su Suergiu mine, and flows directly into the Flumendosa River. Water from the Flumendosa River is collected in reservoirs, which supply water for agricultural and domestic use in the whole area.

Topography is marked by steep slopes (up to 60%), which are covered by degraded Mediterranean *maquis*. Soils at Su Suergiu are characterized by sandy loam to clay loam texture, with 20 to 30% coarse fragments, near-neutral pH, electrical conductivity (EC) values generally below 0.5 mS cm⁻¹, and mean organic carbon in the A horizon of 44 g kg⁻¹ (Cidu et al. 2014). Predominant minerals are quartz, muscovite, illite, biotite, clinocllore, and montmorillonite, with some calcite in the bedrock (Cidu et al. 2014). Antimony concentrations in the soil horizons are from <8 to 4400 mg kg⁻¹ (Cidu et al. 2014), and As from 19 to 390 mg kg⁻¹, the higher values being observed in soils close to the slag heaps. Concentrations up to 1700 µg L⁻¹ Sb (Cidu et al. 2014), and 18 µg L⁻¹ As were found in the pore water of soils for the <0.45 µm fraction. Present land use is for livestock, mainly cattle grazing. No information is available on any signs of livestock/cattle being affected by contamination in their feed.

Methods

Solid Materials

To collect data on the foundry wastes, solid materials (3 samples) were collected in May 2014 at the slag heap close to the SU1 location (see Fig. 1). Solid samples are made up of slag pebbles (size range: 1 to 10 cm) mixed with coarse to fine particles. Solid samples were analyzed as such (bulk solid) and by separating the slag pebbles. Minerals in the bulk solids and individual slag pebbles were identified using an X-ray diffractometer (XRD, Panalytical X'pert Pro). The XRD patterns were collected in the 5–70° 2θ angular range, using the Ni-filter monochromatised Cu-Kα1 radiation (at λ = 1.54060 Å) at 40 kV and 40 mA, and the X'Celerator detector. The detection limit of the XRD was about 3%. The slag pebbles were investigated

by scanning electron microscopy (SEM, FEI Quanta 200); semi-quantitative chemical analyses were carried out by X-ray EDS.

In previous studies, bulk solids collected at the waste heaps were sieved to <2 mm size and submitted for leach testing using ultrapure water (MILLI-Q >18 MΩ cm), the solid to water ratio was 1: 20, and the leachate was analyzed after 2 and 24 h of interaction (Cuzzocrea 2007).

Water Samples

Hydrogeochemical surveys conducted from 2005 to 2015 produced time-series data and downstream profiles of water chemistry at 46 sites (Fig. 1). Samples were collected from: springs and streams upstream of and unaffected by the mined area (Group 1; 18 sampling sites); water from adits and streams in the mined area (Group 2a; 11 sampling sites); water draining the slag heaps (Group 2b; 4 sampling sites); streams downgradient from the slag drainages (Group 3; 4 sampling sites); and water in the Flumendosa River downstream from its confluence with the contaminated water (Group 4; 9 sampling sites). At selected sites, water sampling was repeated under different seasonal conditions over the period 2005–2015, resulting in a total of 99 samples.

The flow was calculated by measuring water velocity several times at different points along a specific section. Taking into account that the bed of large streams is very rough, flow measurements under high flow condition are subject to large errors. However, a comparison of our data collected on 23 May 2012 with those taken the same day by the Flumendosa River Authority (personal communication, Ente Autonomo del Flumendosa, Cagliari, Italy) showed that flows were within 20% of each other. On-site measurements include temperature, pH, redox potential (Eh), EC, and alkalinity. The Eh was measured with a platinum combination electrode, and values were checked against ZoBell's solution (Nordstrom 1977).

Analyses were done at the analytical laboratories of the University of Cagliari. Alkalinity was measured both in the field by titration with hydrochloric acid (indicator: methyl orange) and in the laboratory with the Gran function plot method. Alkalinity was chiefly attributed to the HCO₃⁻ ion, since the CO₃²⁻ ion was always undetectable and the contribution of non-carbonate species was negligible. The water was filtered through 0.45 µm pore-size filters, on site immediately upon collection. A filtered aliquot was analyzed by ion chromatography (IC, Dionex ICS3000). A filtered aliquot was also used to determine dissolved organic carbon (DOC) in water collected in the 23 July 2013 survey (Cidu et al. 2014). An aliquot filtered into a pre-cleaned high-density PE bottle was acidified with supra pure HNO₃ (1%, v/v) for analysis by inductively-coupled plasma mass spectrometry (ICP-MS, PE- ElanDRC). An aliquot filtered

and acidified with supra pure HCl (0.5%, v/v) was used for As determination. At selected sites, an unfiltered aliquot was collected, and filtration tests were performed on site using both 0.45 and 0.01 μm pore-size filters. Filtration tests were carried out to distinguish the colloidal fraction from the truly dissolved fraction. Because Fe and Al were often below detection limit by either ICP-MS or inductively-coupled plasma optical emission spectrometry (ICP-OES, ARL3520) using external calibration, metals were determined in the samples collected on 05 Dec. 2014 by the standard addition method (Cidu 2000).

Concentrations of Sb were determined by ICP-MS, using the ^{121}Sb and ^{123}Sb isotopes, and Rh as an internal standard. Concentrations of As were determined by hydride generation on-line with an ICP-MS (Cidu 1996). For concentrations $>50 \mu\text{g L}^{-1}$, Sb and As were also determined by ICP-OES. Concentrations of Sb(III) and As(III) were determined by anodic stripping voltammetry (ASV, Metrohm 797 VA Computrace) with a hanging mercury drop electrode (Cidu et al. 2015) and a gold electrode, respectively. The solutions SRM1643e supplied by the U.S. National Institute of Standard & Technology (Gaithersburg, MD), and EnviroMAT ES-L-2 and EP-H-3 supplied by SCP Science (St. Laurent, QC), were used to evaluate analytical uncertainties: $<5\%$ for Sb and $<10\%$ for As.

Modeling

The WATEQ4F program was used to calculate the quality of water analyses. It was verified by plotting the conductivity imbalance, i.e. $\text{SCI} = [(\text{EC}_{\text{calculated}} - \text{EC}_{\text{measured}})/\text{EC}_{\text{measured}}] \times 100$, with respect to the speciated charge imbalance, i.e. $\text{C.I.} = [(\sum \text{cations} - \sum \text{anions}) / (\sum \text{cations} + \sum \text{anions})] \times 100$ (McCleskey et al. 2011 and references therein). The charge imbalance was within $\pm 10\%$.

Speciation and equilibrium calculations were carried out with Visual MINTEQ and the Stockholm Humic Model (SHM; Gustafsson 2001) that includes organic species for Sb in the database, and EQ3, version 8.0 (Wolery and Jarek 2003), with updated thermodynamic data for Sb, as explained in Cidu et al. (2014). The saturation state of an aqueous solution with respect to the i^{th} solid phase is indicated by the saturation index, SI_i defined by the equation (Langmuir 1997; Nordstrom and Campbell 2014):

$$\text{SI}_i = \log \frac{Q_i}{K_i}$$

where Q_i stands for the corresponding ionic activity product in the aqueous solution and K_i refers to the solubility product of the i^{th} solid phase.

Results

Solid Characteristics and Leaching Tests

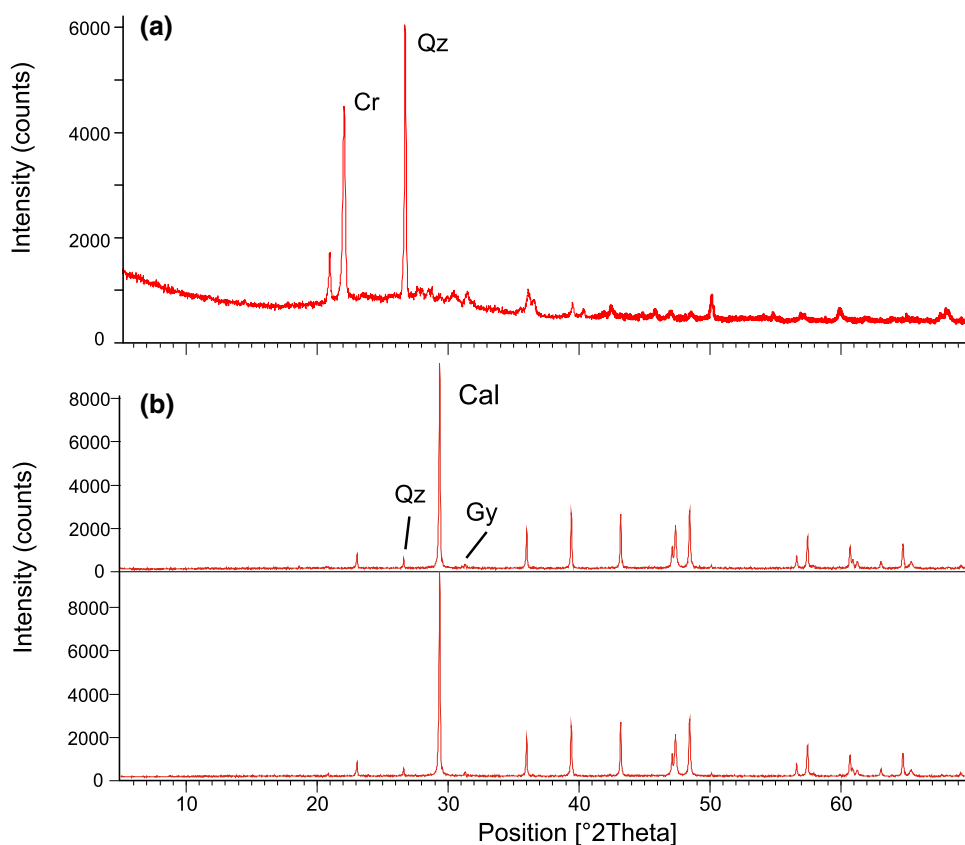
In the slag heaps, weighted average values of Sb and As were $59,300$ and 666 mg kg^{-1} , respectively (IGEA 2009). In this study, mineral phases hosting Sb and/or As were not identified by XRD in the bulk material nor in the slag. Mineral phases recognized by XRD were quartz and cristobalite (SiO_2 phase at high temperature) in the slag pebbles (Fig. 2a), and calcite, quartz, and gypsum in the bulk solids (Fig. 2b). These results confirm previous XRD investigations carried out on 11 solid samples collected at the Su Suergiu slag heaps (Cabras 2006). Detailed SEM images of the slag pebbles show grayscale areas (e.g. square 1 in Fig. 3a) and many bright spots (e.g. square 2 in Fig. 3a). The EDS spectrum of grayscale areas shows high peaks of Si and O, followed by Ca, Al, Fe, and Mg (Fig. 3b). The bright spots generally have globular shape with size between 10 and 30 μm (Fig. 3c), and the corresponding EDS spectrum shows high peaks of Sb and O (Fig. 3d), probably indicating Sb-oxide phases.

Leaching tests carried out on the bulk slag materials showed high Sb and As in the leachate (Cidu 2011) together with high SO_4^{-2} and Fe. High Sb may derive from the dissolution of Sb-oxides, as suggested by the EDS spectrum (Fig. 3d). High As may derive from the dissolution of arsenopyrite, although As peaks were not identified by EDS. More detailed mineralogical characterization on the slag and other wastes would better address this aspect, but it was beyond the scope of this study.

Water Characteristics

Summary statistics of physical and chemical parameters in each water group are reported in Table 1, where Group 1 samples are from upstream of the mine, Group 2 are in the immediate vicinity of the mine, Group 3 are from the Rio Sessini and Rio Ciurixeda, and Group 4 are from the Flumendosa River after confluence with the mine-contaminated water. All of the water samples had a circumneutral pH and oxidizing Eh values. The chemical composition of spring water collected under different seasonal conditions showed small variations (Supplemental Table 1). The relative proportion of dissolved major ions (Ca^{2+} , Mg^{2+} , Na^+ , K^+ , HCO_3^- , SO_4^{-2} , Cl^-) was nearly constant over time in each group (Fig. 4), except Groups 2a and 2b that vary markedly by dilution. The relative proportion of dissolved major ions in the water collected in the Flumendosa River did not vary substantially before (MU92) and after (SU11) the Rio Ciurixeda confluence, but median SO_4^{-2} in Group 4 was higher than median SO_4^{-2} in Group 1 (Table 1). However, SO_4^{-2} concentrations in Group 4 were

Fig. 2 XRD patterns in the slag pebbles (a) and bulk solid samples (b) collected at Su Suergiu (Cal calcite, Cr cristobalite, Gy gypsum; Qz quartz)



below the Italian limit established for drinking water (i.e. 250 mg L^{-1} ; GURI 2006), under both high and low flow conditions (Supplemental Table 1).

Median EC values in waters of Group 1 and Group 4 were below 0.6 mS cm^{-1} , whereas they increased up to 3.8 mS cm^{-1} in Group 2 samples because of the high concentrations of SO_4^{2-} , Ca^{2+} , and Mg^{2+} , and also Na^+ in the Group 2b slag drainage samples (Table 1 and Supplemental table 1). The Group 2b samples were also distinguished by median silica higher than the other groups.

The median Sb and As concentrations (1.7 and $1.6 \text{ } \mu\text{g L}^{-1}$, respectively) in Group 1 samples were below the limits established for drinking water, but relatively high with respect to median values in uncontaminated Sardinian surface water ($0.3 \text{ } \mu\text{g L}^{-1}$ Sb and $1 \text{ } \mu\text{g L}^{-1}$ As; Cidu and Frau 2009), and median values in Sardinian groundwater, estimated at $0.5 \text{ } \mu\text{g L}^{-1}$ Sb (Biddau 2012) and $0.6 \text{ } \mu\text{g L}^{-1}$ As (Biddau and Cidu 2013), suggesting that concentrations of these elements in the Group 1 waters reflect high values of local background due to the geological setting in the Gerrei mining district. The samples collected in the mined area (Group 2a) were characterized by highly variable concentrations of Sb (median: $316 \text{ } \mu\text{g L}^{-1}$), whereas median As ($2.0 \text{ } \mu\text{g L}^{-1}$) was similar to that observed in Group 1 waters (Supplemental Table 1). In the mined area, high concentrations of Sb

were accompanied with high As in the slag drainage (Group 2b, Fig. 5). The highest Sb and As concentrations were observed in waters flowing from the slag materials (Group 2b) derived from the processing of Sb ore, therefore, the slag materials were the main source of Sb and As in water at Su Suergiu (Table 1).

When detected, the maximum ($147 \text{ } \mu\text{g L}^{-1}$) concentration of Sb(III) corresponded to $<2\%$ of total dissolved Sb in the $<0.45 \text{ } \mu\text{m}$ water fraction (Cidu et al. 2015). Speciation modeled by Visual MINTEQ showed that Sb(V) and Sb(III), respectively, occur as $\text{Sb}(\text{OH})_6^-$ (100%) and $\text{Sb}(\text{OH})_3$ (99.9%) aqueous species in the Su Suergiu waters. Arsenic speciation was dominated by the HAsO_4^{2-} species in the studied waters, but aqueous arsenate complexes, such as NaHAsO_4^- and CaAsO_4^- , increased at concentrations above 1 mg L^{-1} As. Detectable concentrations of As(III) ($5\text{--}9 \text{ } \mu\text{g L}^{-1}$) were rarely observed in the SU1 slag drainage, and corresponded to $<1\%$ of total dissolved As in the $<0.45 \text{ } \mu\text{m}$ water fraction. In water where DOC was detected in the range of $1.2\text{--}1.9 \text{ mg L}^{-1}$ (Cidu et al. 2014), aqueous complexes of either Sb or As with DOC were negligible.

In Groups 3 surface waters (i.e. SU20 and MU8) and 4 (i.e. Flumendosa River downstream of the contaminated Rio Ciurixeda), SO_4^{2-} , Sb, and As concentrations decreased at increasing distance downstream from the mine area (Fig. 6). Concentrations of As and Sb in the Group 4

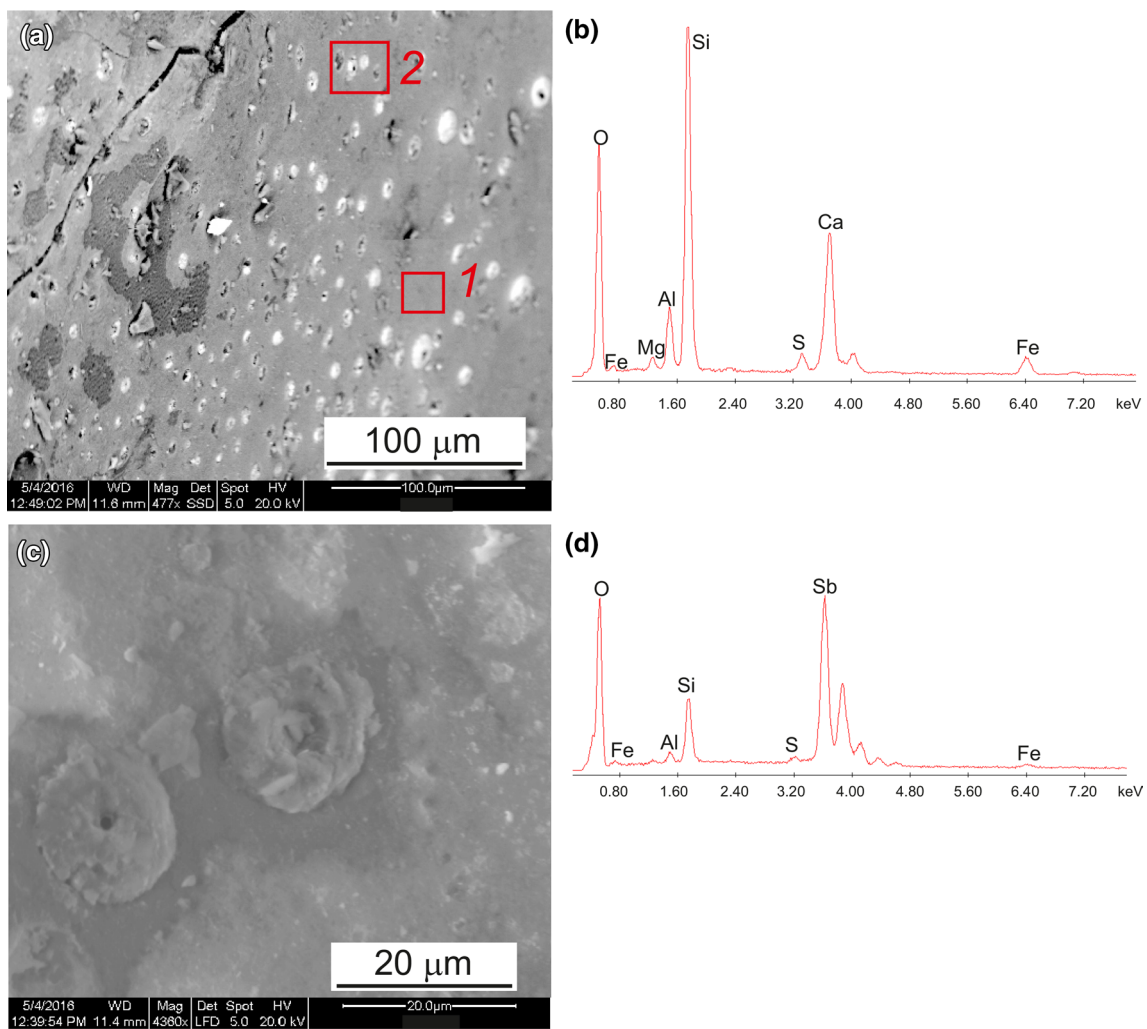
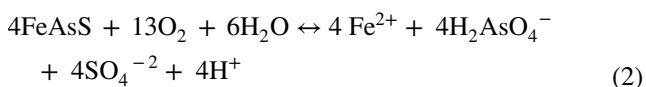
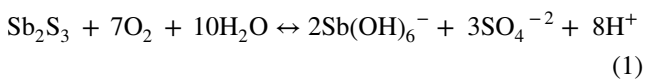


Fig. 3 **a** Backscattered electron image of slag pebble; **b** EDS spectrum of the grey area, *square 1*; **c** secondary electron image of the bright spot, *square 2* and **d** EDS spectrum of the bright spot

waters collected at high flow were higher than at low flow (Fig. 7).

Discussion

The SO_4^{-2} , As, and Sb may be derived from the oxidative dissolution of sulfide minerals, such as pyrite, stibnite (reaction 1, Leverett et al. 2012), and arsenopyrite (reaction 2, Craw et al. 2003):



In Group 2a water, As and Sb remained lower than in Group 2b, even at high SO_4^{-2} concentrations, suggesting

more complete breakdown of sulfide minerals to more soluble phases.

Consistent with reaction (2) and EDS observations (Fig. 3b, d), the slag materials submitted for leaching tests released Fe in the leachate. However, Fe in the slag drainages was very low, which is consistent with the oxidizing condition and near neutral to slightly alkaline pH observed at Su Suergiu that favor Fe precipitation.

The oxidation of sulfide minerals would normally decrease the pH but for the dissolution of the Na-carbonate that was used in the ore processing. Dissolution of Na-carbonate also promotes the precipitation of calcite, which easily reaches saturation and limits Ca^{2+} concentrations. According to MINTEQ, gypsum supersaturation would not be reached, but gypsum precipitation may occur due to high evaporation, especially in the Group 2 waters (Fig. 8). Indeed, gypsum was recognized by XRD in the bulk slag materials (see Fig. 2b).

Table 1 Summary statistics of physical characteristics and concentrations of major components, antimony and arsenic determined in water samples collected in surveys from 2005 to 2015

	T, °C	pH	Eh, V	EC, mS cm ⁻¹	Ca, mg L ⁻¹	Mg, mg L ⁻¹	Na, mg L ⁻¹	K, mg L ⁻¹	HCO ₃ ⁻ , mg L ⁻¹	Cl ⁻ , mg L ⁻¹	SO ₄ ⁻² , mg L ⁻¹	SiO ₂ , mg L ⁻¹	Sb, µg L ⁻¹	As, µg L ⁻¹
Group 1 waters upstream mine (n=34)														
Min	8	6.1	0.33	0.19	6.7	4.1	22	0.5	34	38	8	2.4	0.2	0.2
Max	26	8.2	0.51	1.16	174	38	42	3.1	290	73	346	28	8.9	9.5
Median	16	7.8	0.43	0.51	56	16	30	1.6	187	54	46	8.0	1.7	1.6
Mean	16	7.7	0.44	0.52	57	17	31	1.7	166	54	64	9.0	2.4	2.0
SD	4.5	0.5	0.04	0.20	33	8.9	4.9	0.6	67	10.4	61	4.9	2.2	2.1
Group 2a mine waters (n=13)														
Min	8	7.0	0.17	0.41	41	11	26	1.5	98	43	48	4.6	4.7	0.5
Max	19	8.2	0.51	3.19	560	160	64	8.2	583	90	1900	10.1	890	20
Median	15	7.8	0.44	1.00	165	38	38	3.0	244	55	377	8.1	316	2.0
Mean	15	7.7	0.42	1.43	256	59	40	3.3	258	62	650	7.8	370	5.4
SD	4.0	0.4	0.08	0.88	188	50	10	1.8	126	16	631	1.6	285	6.4
Group 2b slag drainages (n=19)														
Min	9	7.1	0.32	1.46	243	47	44	2	264	46	663	10	4400	300
Max	25	8.5	0.49	3.75	450	109	600	21	651	76	1800	49	30,000	16,000
Median	19	8.0	0.43	2.39	337	63	163	8.8	395	59	1015	18	12,800	3900
Mean	19	8.0	0.42	2.35	327	66	208	9.4	419	57	1091	24	12,205	5558
SD	4.2	0.4	0.05	0.61	61	17	159	5.0	96	6.9	290	13	7142	4886
Group 3 waters downstream slag (n=14)														
Min	8	7.6	0.29	0.71	82	18	37	3.1	186	56	131	2.9	800	49
Max	22	8.3	0.50	1.20	176	30	69	6.1	415	106	295	15.7	2345	226
Median	18	7.9	0.46	1.04	149	24	50	4.1	281	76	234	8.8	1515	61
Mean	17	7.9	0.44	0.99	143	24	51	4.3	289	78	224	9.1	1459	75
SD	4.2	0.2	0.06	0.16	28	4	10	0.9	69	15	53	4.0	390	46
Group 4 Flumendosa downstream MU8 (n=19)														
Min	8	7.3	0.28	0.41	38	16	26	1.5	129	48	42	1.7	14	1.3
Max	27	8.3	0.50	0.77	84	31	41	3.0	236	74	113	8.0	51	13
Median	18	8.0	0.46	0.56	60	21	32	2.2	197	56	69	5.6	25	3.4
Mean	17	8.0	0.44	0.58	60	22	32	2.1	195	56	70	5.4	27	4.1
SD	5.3	0.2	0.06	0.08	9.3	3.3	3.7	0.4	26	6.2	14	2.0	10	2.7

Water samples were filtered through 0.45 µm pore-size filters

Eh redox potential, *EC* electrical conductivity, *n* number of samples, *Min.* minimum value, *Max* maximum value, *SD* standard deviation

Fig. 4 Piper diagram showing the relative proportion of major ions in the studied waters in the surveys carried out from 2005 to 2015

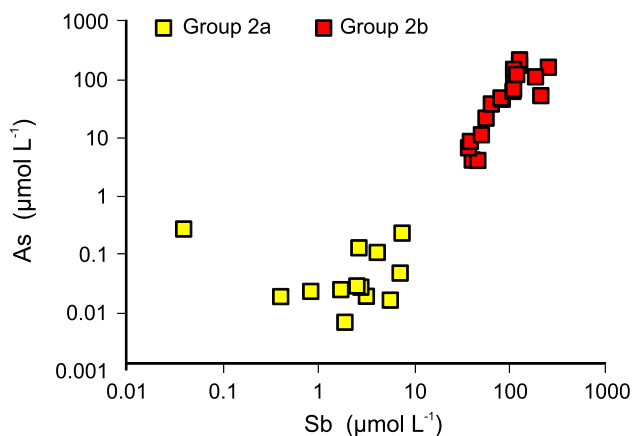
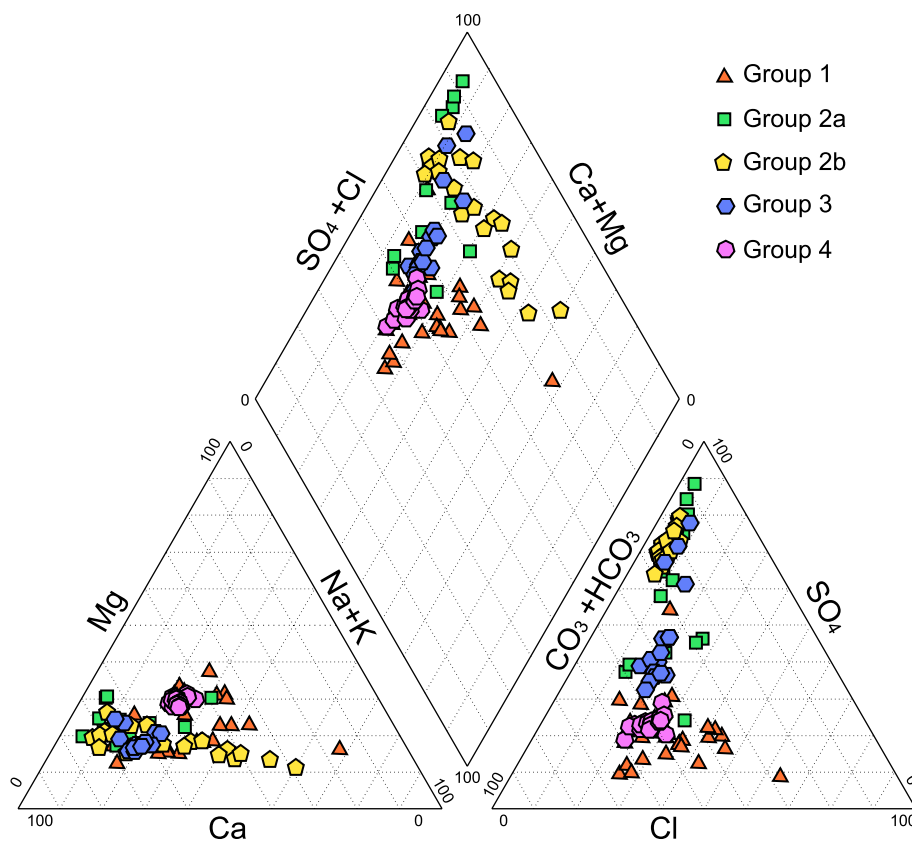


Fig. 5 Plot showing As versus Sb in mine waters (*Group 2a*) and slag drainages (*Group 2b*)

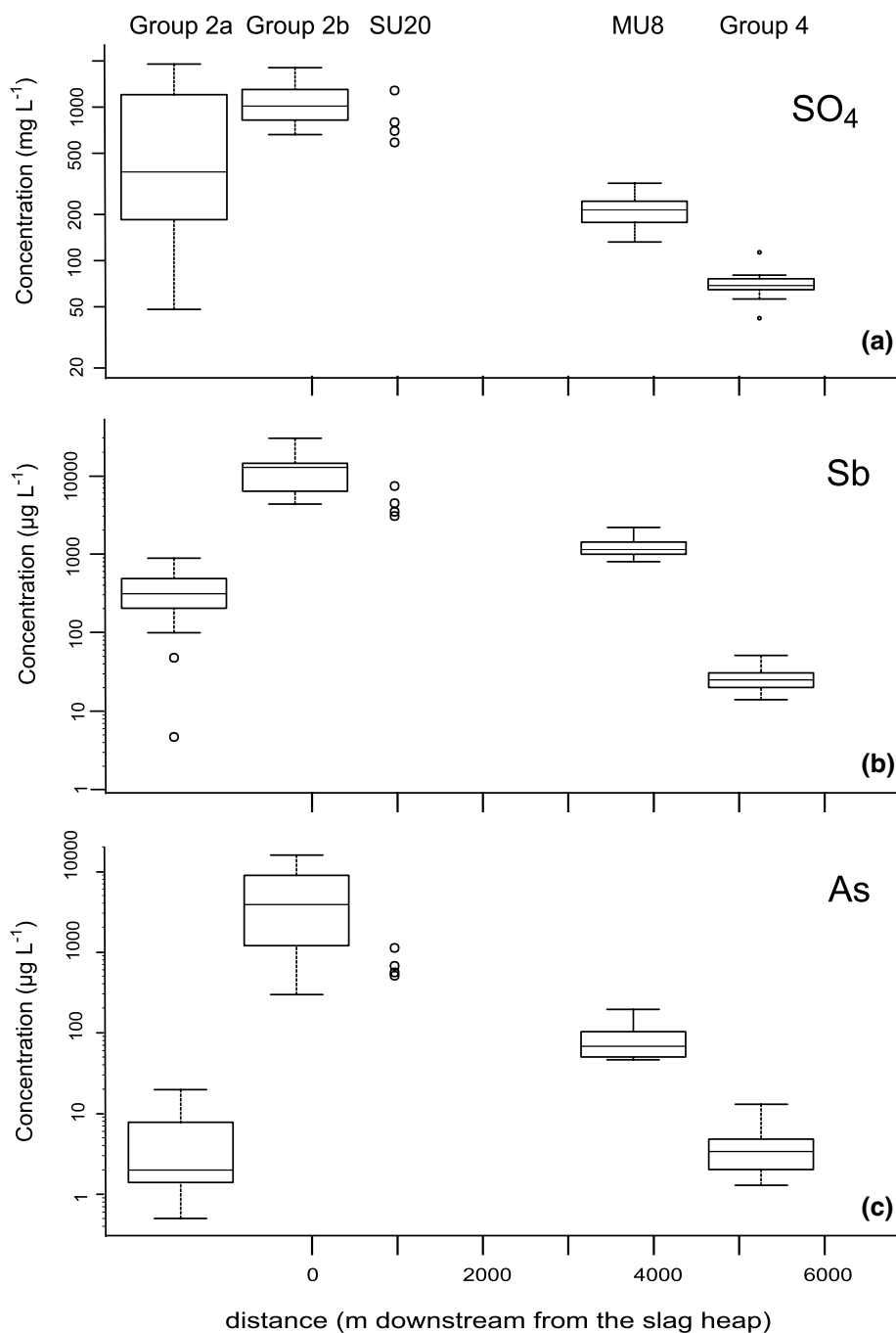
Other than the oxidative dissolution of stibnite, Sb might be released by dissolution of other Sb-bearing solid phases, such as valentinite [Sb₂O₃] and/or tripuhyite [FeSbO₄], probably contained in the slag materials (Fig. 3d). Another alternative is that after the stibnite oxidizes, the Sb reprecipitates as a secondary mineral, while the SO₄²⁻ remains in solution. If the latter is the main reason for the Sb/SO₄²⁻

molar ratios being much lower than that of stibnite, then the greatest attenuation of Sb may occur at the source.

To identify possible attenuation processes, such as precipitation of Sb-bearing solid phases, the species calculation was performed by EQ3 on the slag drainage sample (SU2, collected in 30 October 2012) that showed the highest contents of SO₄²⁻, Sb, and As in the Su Suergiu waters (Supplemental Table 1). The results indicate undersaturation with respect to the Sb- and As-bearing solid phases.

As mentioned earlier, the amount of Sb(III) in the Su Suergiu waters was low, probably because the Sb(III) was being rapidly oxidized and/or adsorbed. Because abiotic aqueous Sb(III) oxidation is so slow as to be undetectable (Gmelin 1908), this oxidation must be catalyzed by microbial activity. Aqueous Sb(III) oxidation has been demonstrated by a few microorganisms (Oremland 2016), but more research is warranted. Dissolved Sb(III) might also have been removed by sorption due to its high affinity with the particulate phase (Leuz et al. 2006; Thanabalasingam and Pickering 1990; Wu et al. 2011). In contrast, sorption of Sb(V)-bearing species onto solid phases appears unlikely given the pH and oxidizing conditions, which allows dispersion of Sb for a long distance downstream. Moreover, the high HAsO₄²⁻ and bicarbonate concentrations would compete for sorption sites, thus hampering sorption of

Fig. 6 Box-plots of dissolved SO_4^{-2} (a), Sb (b) and As (c) in waters versus distance from the mine area to the Flumendosa River



$\text{Sb}(\text{OH})_6^-$ species onto sediment surfaces (Desbarats et al. 2011).

Mass balances were obtained downstream of the mined area by comparing the loads of conservative components (Na^+ , Cl^- , and SO_4^{-2}) and Sb and As (all determined in the $<0.45 \mu\text{m}$ fraction) in the Flumendosa River before (MU92) and after (SU11) the Rio Ciurixeda confluence (Table 2). Results suggest conservative behavior, although a larger error is expected for high flow than for low flow measurements. The loads for major components

were nearly constant upstream (MU92+MU8) and downstream of the confluence (SU11), as were the Sb and As loads, suggesting that the main abatement of dissolved Sb, As, and SO_4^{-2} is by dilution. However, under some high flow conditions (05 Dec. 2014), the Sb load downstream of the confluence (SU11) was substantially greater than upstream (Table 2). There are two possible explanations for this. Sorption of $\text{Sb}(\text{OH})_6^-$ onto particulate phases can contribute to Sb transport, but it takes a very high flow to add enough suspended particles to make a difference. To verify

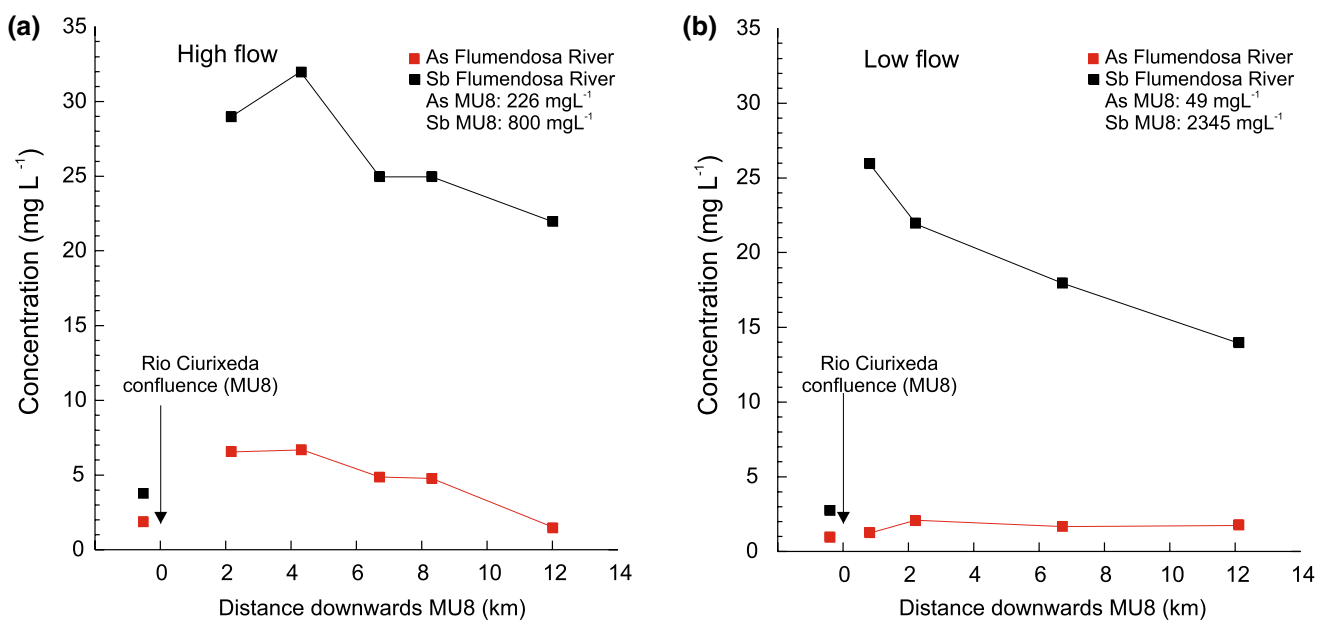


Fig. 7 Concentrations of As and Sb in the Flumendosa River under high flow (a) and low flow (b) conditions

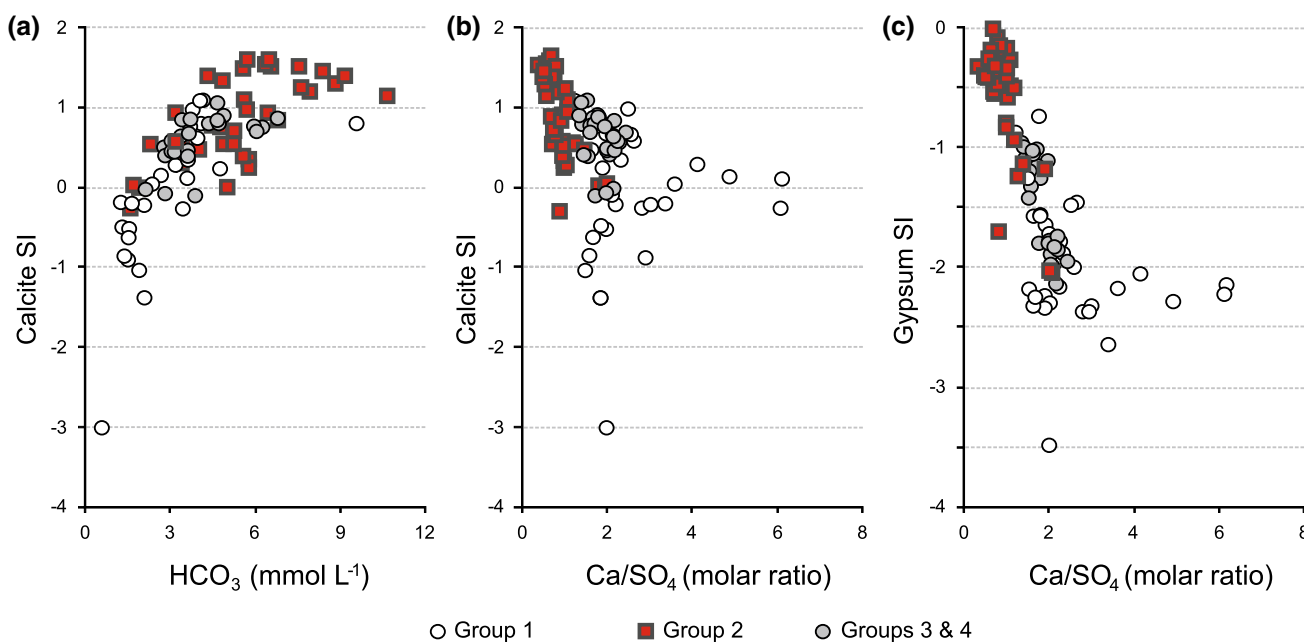


Fig. 8 a Plot of calcite saturation index (SI) versus HCO₃⁻ concentration. b Plot of calcite saturation index (SI) versus Ca²⁺/SO₄⁻² molar ratio. c Plot of gypsum saturation index (SI) versus Ca²⁺/SO₄⁻² molar ratio

this hypothesis, filtration tests were carried out on 05 Dec. 2014 water samples (Table 3; Fig. 9). The data indicate that the dissolved Sb load in the Flumendosa River downstream of the Rio Ciurixeda confluence might have increased due to sorption onto Fe- and Al-bearing colloidal phases. The other possibility is that under high-flow conditions,

riverbank and bed sediment particles were remobilized and transported downstream.

It is worth noting that dispersed slag pebbles occur 4 km downstream from the mine area until the confluence of Rio Ciurixeda with the Flumendosa River. This may contribute to the persistently high concentrations of Sb and As in the

Table 2 Comparison of loads of Sb, As and conservative elements in the Flumendosa River before (A: MU92) and after (C: SU11) the Rio Ciurixeda (B: MU8) confluence under different seasons

Date	Sample	Flow, L s ⁻¹	Sb, mg s ⁻¹	As, mg s ⁻¹	Cl ⁻ , g s ⁻¹	SO ₄ ⁻² , g s ⁻¹	Na, g s ⁻¹
23/05/2012	A MU92	1000	3.9	2.9	53	72	33
	B MU8	20	30.8	1.2	1.5	3.86	0.98
	C SU11	1100	31.9	3.9	58.3	82.5	35.2
	(A+B)/C	0.93	1.09	1.07	0.93	0.92	0.97
28/02/2013	A MU92	2700	5.13	4.1	130	108	75.6
	B MU8	35	56	2.8	2.1	4.7	1.3
	C SU11	2900	55.1	5.8	139	124.7	75.4
	(A+B)/C	0.94	1.11	1.18	0.95	0.90	1.02
09/01/2014	A MU92	3000	6.3	4.8	153	159	84
	B MU8	100	160	7.3	6.5	15.2	3.7
	C SU11	3200	163	10.9	163.2	185.6	89.6
	(A+B)/C	0.97	1.02	1.11	0.98	0.94	0.98
05/12/2014	A MU92	4500	15.3	10.4	255	252	126
	B MU8	60	110	3.2	4.6	15.1	2.8
	C SU11	4600	221	14.7	245	282	129
	(A+B)/C	0.99	0.57	0.92	1.06	0.95	1.00

Table 3 Filtration tests carried out on waters sampled on 05/12/2014; NF=not filtered, F=filtered through 0.45 µm pore-size filter, and FF=filtered through 0.01 µm pore-size filter

Sample	Fe, µg L ⁻¹	Al, µg L ⁻¹	As, µg L ⁻¹	Sb, µg L ⁻¹
MU92 NF	137	61	3.1	3.14
MU92 F	24	7	2.3	3.37
MU92 FF	21	9	2.3	2.46
MU8 NF	23	10	55	1845
MU8 F	2	4	53	1830
MU8 FF	2	5	57	1840
SU11 NF	94	35	4.3	64.5
SU11 F	24	8	3.2	48.0
SU11 FF	26	11	2.8	48.1

Rio Ciurixeda (MU8) under low- and high-flow conditions. The high Sb and As content at low-flow despite little input from the mined area, is likely due to evaporative concentration. At high-flow, the effect of dilution may be partly compensated for by the interaction of water and slag materials dispersed downstream of the mined area.

Figure 10 shows Sb and As concentrations in the Flumendosa River upstream and downstream of the Rio Ciurixeda confluence from surveys conducted in 2005 to 2015. The As concentration only exceeded the EU and WHO established limit (10 µg L⁻¹ As) in 2010, whereas the Sb in the Flumendosa River downstream of the contaminated stream always exceeded the EU limit (5 µg L⁻¹ Sb), and frequently exceeded the WHO limit (20 µg L⁻¹ Sb), indicating that recent actions aimed at retaining runoff from the slag heaps is not sufficient to mitigate the impact of the contaminated water on the Flumendosa River.

Conclusions

Mining and mineral processing of Sb at the abandoned Su Suergiu mine in southern Sardinia has contributed substantial quantities of SO₄⁻², Sb, and As to downstream surface waters. Sulfate was shown to be conservative; downstream from the mined area, dilution decreased SO₄⁻² concentrations in the Flumendosa River to below regulatory limits. The main source of the Sb and As was drainage water from slag on the mine site, with minor amounts contributed by adit drainage. This study also demonstrated the important influence that a strong base such as Na-carbonate from the foundry wastes can have on mobilizing Sb and As and keeping them in solution.

There is no clear evidence of natural attenuation due to precipitation of Sb- and As-bearing phases, but it is not possible to exclude this entirely, especially near the source of contamination. Sorption of Sb and As on particulate/colloidal phases may occur in surface waters under very high flow conditions. Downstream of the mined area, the natural abatement of Sb and As concentrations is mainly by dilution, rather than by sorption onto bed sediment. Despite natural dilution, the Rio Ciurixeda discharges strongly contaminated water (up to 14 kg Sb per day and 0.6 kg As per day, under high flow conditions) into the Flumendosa River. This major water source is used for agricultural and domestic purposes. Therefore, further remedial action is needed to reduce Sb and As input into surface waters and nearby groundwater, as the retaining wall currently in place is insufficient. Remediation priorities should address the environmental impact of the main source of contamination, i.e. the Sb-As-rich heaps. Construction of drainage

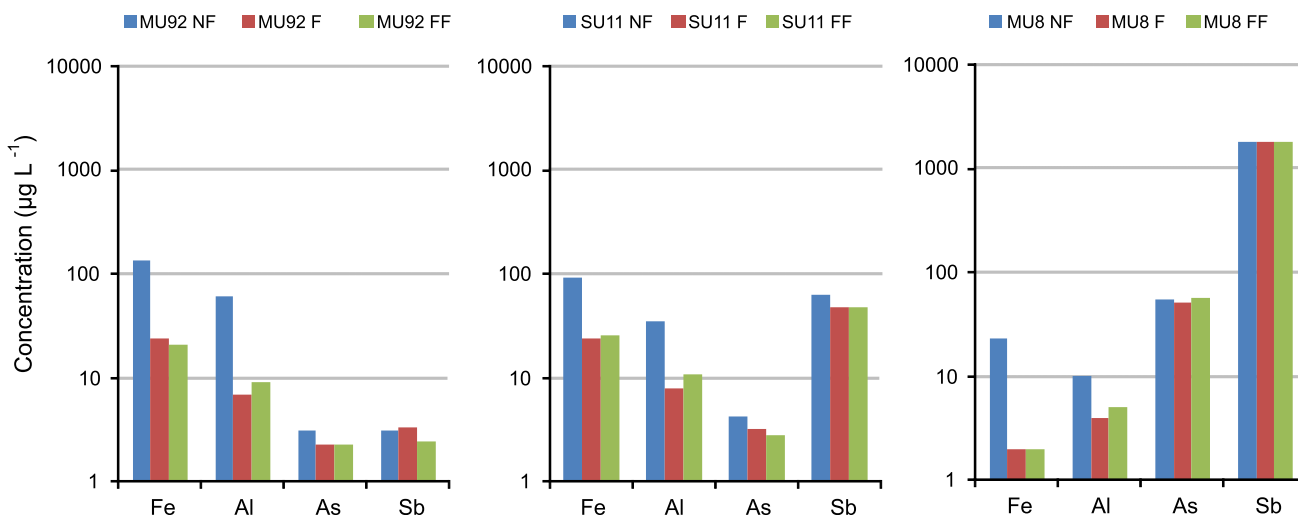


Fig. 9 Comparison of Fe, Al, As, and Sb concentrations determined in different aliquots. *NF* not filtered, *F* water filtered through 0.45 µm pore-size filter, and *FF*=water filtered through 0.01 µm pore-size filter

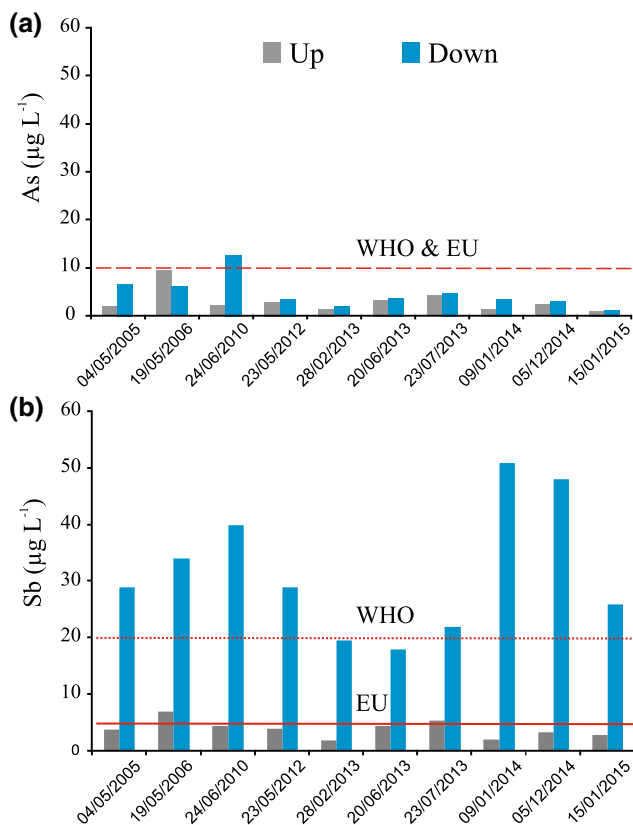


Fig. 10 Comparison of As (a) and Sb (b) concentrations in the Flumendosa River upstream (*up*) and downstream (*down*) the Rio Ciurixeda confluence. Lines indicate the WHO and EU limits for As and Sb in drinking water

ways to divert rainfall and runoff from the heaps should help reduce the interaction of water with the contaminated materials.

Acknowledgements We thank the Ministero Università Ricerca Scientifica Tecnologica (PRIN 2009J425AL, Coordinator R Cidu), the University of Cagliari, and the Regione Autonoma della Sardegna (PO Sardegna FSE 2007–2013, L.R.7/2007, R Biddau) for financial support. Thanks to G De Giudici for helping with the SEM analyses. Any use of trade, firm, or product names is for descriptive purposes only and does not imply endorsement by the U.S. Government.

References

Amat di San Filippo P (2014) L’Antimonio in Sardegna e la Fonderia di Villasalto. <http://www.academiasarda.it/2014/04/lantimonio-in-sardegna-e-la-fonderia-di-villasalto-di-paolo-amat-di-san-filippo/> (accessed May 2016)

Asaoka S, Takahashi Y, Araki Y, Tanimizu M (2012) Comparison of antimony and arsenic behavior in an Ichinokawa River water–sediment system. *Chem Geol* 334:1–8

Ashley PM, Craw D, Graham BP, Chappell DA (2003) Environmental mobility of antimony around mesothermal stibnite deposits, New South Wales, Australia and southern New Zealand. *J Geochem Expl* 77:1–14

Beauchemin S, Kwong YTJ, Desbarats AJ, MacKinnon T, Percival JB, Parsons MB, Pandya K (2012) Downstream changes in antimony and arsenic speciation in sediments at a mesothermal gold deposit in British Columbia, Canada. *Appl Geochem* 27:1953–1965

Bhattacharya P, Welch AH, Stollenwerk KG, McLaughlin MJ, Bundschuh J, Panaullah G (2007) Arsenic in the environment: Biology and Chemistry. *Sci Total Environ* 379:109–120

Biddau R (2012) Approccio geochimico-statistico per la valutazione del background geochimico nelle acque sotterranee. Applicazioni agli acquiferi della Sardegna. FSE 2007–2013, LR 7/2007, Regione Autonoma Sardegna, Cagliari (in Italian)

Biddau R, Cidu R (2013) Groundwater contamination: environmental issues and case studies in Sardinia (Italy). In: Scozzari A, Dot-sika E (eds) Threats to the quality of groundwater resources: prevention and Control, The handbook of environmental. chemistry. Springer-Verlag, Berlin

- Cabras R (2006) Studi idrogeochimici e mineralogici nell'area della miniera abbandonata di Su Suergiu (Villasalto). Tesi di Laurea in Scienze Geologiche, Università di Cagliari, p 97 (in Italian)
- Carmignani L, Coccozza T, Ghezzi C, Pertusati PC, Ricci CA (1986) Outlines of the Hercynian basement of Sardinia. In: Carmignani L, Coccozza T, Ghezzi C, Pertusati PC, Ricci CA (Eds), Guide book to the excursion on the Palaeozoic basement of Sardinia. IGCP Newsletter 5, Special Issue, pp 11–21, Pacini Editore, Pisa
- Carvalho PCS, Ana MR, Neiva AMR, Silva MVG, Ferreira da Silva EA (2014) Geochemical comparison of waters and stream sediments close to abandoned Sb–Au and As–Au mining areas, northern Portugal. *Chem Erde* 74:267–283
- Casiot C, Ujevic M, Munoz M, Seidel JL, Elbaz-Poulichet F (2007) Antimony and arsenic mobility in a creek draining an antimony mine abandoned 85 years ago (Upper Orb Basin, France). *Appl Geochem* 22:788–798
- Cidu R (1996) Inductively coupled plasma—mass spectrometry and—optical emission spectrometry determination of trace elements in water. *Atom Spectrosc* 17:155–162
- Cidu R (2000) Trace elements: Li, Be, B, Al, V, Cr, Co, Ni, Se, Sr, Ag, Sn, Ba, and Tl. In: Nollet L (ed) Handbook of water analysis, Ch 23. Marcel Dekker, New York, pp 459–482
- Cidu R (2011) Mobility of aqueous contaminants at abandoned mining sites: insights from case studies in Sardinia with implications for remediation. *Environ. Earth Sci* 64:503–512
- Cidu R, Frau F (2009) Distribution of trace elements in filtered and non filtered aqueous fractions: Insights from rivers and streams of Sardinia (Italy). *Appl Geochem* 24:611–623
- Cidu R, Frau F, Tore P (2011) Drinking water quality: Comparing inorganic components in bottled water and Italian tap water. *J Food Compos. Analysis* 24:184–193
- Cidu R, Biddau R, Dore E, Vacca A, Marini L (2014) Antimony in the soil–water–plant system at the Su Suergiu abandoned mine (Sardinia, Italy): strategies to mitigate contamination. *Sci Total Environ* 497–498:319–331
- Cidu R, Biddau R, Dore E (2015) Determination of trace of Sb(III) using ASV in Sb-rich water samples affected by mining. *Anal Chim Acta* 854:34–39
- Council of the European Union (1998) Council Directive 98/83/EC of 3 November 1998 on the quality of water intended for human consumption. *Off J L* 330(05/12/1998):35–54
- Craw D, Falconer D, Youngson JH (2003) Environmental arsenopyrite stability and dissolution: theory, experiment, and field observations. *Chem Geol* 199:71–82. doi:10.1016/S0009-2541(03)00117-7
- Cuzzocrea C (2007) Studio idrogeochimico e mineralogico delle aree minerarie di Su Suergiu (Villasalto) e Monte Narba (San Vito). Tesi di Laurea in Scienze Geologiche, Università di Cagliari, pp 76 (in Italian)
- Desbarats AJ, Parsons MB, Percival JB, Beauchemin S, Kwong Y TJ (2011) Geochemistry of mine waters draining a low-sulfide, gold-quartz vein deposit, Bralorne, British Columbia. *Appl Geochem* 26:1990–2003
- Fawcett SE, Jamieson HE, Nordstrom DK, McCleskey RB (2015) Arsenic and antimony geochemistry of mine wastes, associated waters and sediments at the Giant Mine, Yellowknife, Northwest Territories, Canada. *Appl Geochem* 62:3–17
- Filella M, Belzile N, Chen Y-W (2002a) Antimony in the environment: a review focused on natural water. I. occurrence. *Earth Sci Rev* 57:125–176
- Filella M, Belzile N, Chen Y-W (2002b) Antimony in the environment: a review focused on natural waters II. Relevant solution chemistry. *Earth Sci Rev* 59:265–285
- Filella M, Philippo S, Belzile N, Chen Y, Quentel F (2009) Natural attenuation processes applying to antimony: a study in the abandoned antimony mine in Goesdorf, Luxembourg. *Sci Total Environ* 407:6205–6216
- Frau F, Cidu R, Arda C (2012) Short-term changes in water chemistry in the Baccu Locci stream (Sardinia, Italy) affected by past mining. *Appl Geochem* 27:1844–1853
- Funedda A, Naitza S, Tocco S (2005) Caratteri giacimentologici e controlli strutturali nelle mineralizzazioni idrotermali tardo-erciniche ad As-Sb-W-Au del basamento metamorfico paleozoico della Sardegna sud-orientale. *Resoconti Associazione Mineraria Sarda CX:25–46* (in Italian)
- Gmelin L (1908) As, Sb written by F Ephraim (Ed) Gmelin-Kraut's Handbuch der Anorganischen Chemie, Band 3, Abteilung 2, Carl Whiter's Universitatbuchhandlung, Heidelberg, 455
- GURI (2006) Decreto legislativo 3 aprile 2006, n. 152, Norme in materia ambientale. *Gazzetta Ufficiale della Repubblica Italiana* n. 88 del 14-4-2006, suppl. ord. n. 96, Roma (in Italian)
- Gustafsson JP (2001) Modeling the acid-base properties and metal complexation of humic substances with the Stockholm Humic Model. *J Colloid Interface Sci* 244:102–112
- Hiller E, Laninská B, Chovan M, Jurkovič L, Klimko T, Jankulár M, Hovorič R, Šottník P, Flaková R, Ženišová Z, Ondrejková I (2012) Arsenic and antimony contamination of waters, stream sediments and soils in the vicinity of abandoned antimony mines in the Western Carpathians, Slovakia. *Appl Geochem* 27:598–614
- IGEA (2009) Piano di investigazione iniziale dell'area mineraria di "Su Suergiu". IGEA SpA, Campo Pisano (in Italian)
- Kossoff D, Welch MD, Hudson-Edwards KA (2015) Scorodite precipitation in the presence of antimony. *Chem Geol* 406:1–9
- Langmuir D (1997) Aqueous environmental geochemistry. Prentice-Hall, NJ
- Leuz AK, Mönch H, Johnson CA (2006) Sorption of Sb(III) and Sb(V) to goethite: influence on Sb(III) oxidation and mobilization. *Environ Sci Technol* 40(23):7277–7282
- Leverett P, Reynolds JK, Roper AJ, Williams PA (2012) Tripuhyte and schafarzskite: two of the ultimate sinks for antimony in the natural environment. *Mineral Mag* 76:891–902
- Mandal BK (2015) Changing concept of arsenic toxicity with development of speciation techniques. Ch 7. In: Flora SJS (ed) Handbook of As toxicology. Academic Press, Cambridge, MA, pp 175–201
- Masson M, Schäfer J, Blanc G, Dabrin A, Castelle S, Lavaux G (2009) Behavior of arsenic and antimony in the surface freshwater reaches of a highly turbid estuary, the Gironde Estuary, France. *Appl Geochem* 24:1747–1756
- McCleskey RB, Nordstrom DK, Ryan JN (2011) Electrical conductivity method for natural waters. *Appl Geochem* 26:27–29
- Mitsunobu S, Harada T, Takahashi Y (2006) Comparison of antimony behavior with that of arsenic under various soil redox conditions. *Environ Sci Technol* 40:7270–7276
- Nordstrom DK (1977) Thermochemical redox equilibria of ZoBell's solution. *Geochim Cosmochim Acta* 41:1835–1841
- Nordstrom DK, Campbell KM (2014) Modeling low-temperature geochemical processes. In: Drever JI (ed), Surface and Ground Water, Weathering, and Soils, Treatise on Geochemistry, vol 7, HD Holland KK Turekian (Ex Eds), Elsevier, Amsterdam, pp 27–68
- Okkenhaug G, Zhu YG, He J, Xi L, Lei L, Mulder J (2012) Antimony (Sb) and arsenic (As) in Sb mining impacted paddy soil from Xikuangshan, China: differences in mechanisms controlling soil sequestration and uptake in rice. *Environ Sci Technol* 46:3155–3162
- Ondrejková I, Ženišová Z, Flaková R, Krčmář D, Sracek O (2013) The distribution of antimony and arsenic in waters of the

- Dúbrava abandoned mine site, Slovak Republic. *Mine Water Environ* 32:207–221
- Oremland R (2016) Geomicrobial interactions with arsenic and antimony. In: Ehrlich HL, Newman DK, Kappler A (eds) 6th edit. CRC Press, Boca Raton, pp 297–321
- RAS—Regione Autonoma della Sardegna (1998) Nuovo studio dell'idrologia superficiale della Sardegna. Assessorato della Programmazione, Bilancio ed Assetto del Territorio, Ente Autonomo del Flumendosa, Cagliari (in Italian)
- RAS—Regione Autonoma della Sardegna (2003) Piano Regionale di Gestione dei Rifiuti – Piano di Bonifica dei Siti Inquinati, 255 pp. Allegato 5—Schede dei siti minerari dimessi. Cagliari (in Italian)
- RAS—Regione Autonoma della Sardegna (2013) Carta geologica di base della Sardegna in scala 1:25000. <http://www.sardegnaeoportale.it/argomenti/cartageologica.html>. Accessed Oct 2013
- Reimann C, Matschullat J, Birke M, Salminen R (2009) Arsenic distribution in the environment: the effects of scale. *Appl Geochem* 24:1147–1167
- Ritchie VJ, Ilgen AG, Mueller SH, Trainor TP, Goldfarb RJ (2013) Mobility and chemical fate of antimony and arsenic in historic mining environments of the Kantishna Hills district, Denali National Park and Preserve, Alaska. *Chem Geol* 335:172–188
- Roper AJ, Williams PA, Filella M (2012) Secondary antimony minerals: Phases that control the dispersion of antimony in the supergene zone. *Chemie. Erde* 72:9–14
- Smedley PL, Kinniburgh DG (2002) A review of the source, behaviour and distribution of arsenic in natural waters. *Appl Geochem* 17:517–568
- Thanabalasingam P, Pickering WF (1990) Specific sorption of antimony (III) by the hydrous oxides of Mn, Fe and Al. *Water Air Soil Poll* 49(1–2):175–185
- Wang X, He M, Xi J, Lu X (2011) Antimony distribution and mobility in rivers around the world's largest antimony mine of Xikuangshan, Hunan Province, China. *Microchemical J* 97: 4–11
- WHO (2011) Guidelines for drinking-water quality. 4th edit, World Health Organization, Geneva
- Willis SS, Haque SE, Johannesson KH (2011) Arsenic and antimony in groundwater flow systems: a comparative study. *Aquat Geochem* 17:775–807
- Wilson SC, Lockwood PV, Ashley PM, Tighe M (2010) The chemistry and behaviour of antimony in the soil environment with comparisons to arsenic: a critical review. *Environ Poll* 158:1169–1181
- Wolery TW, Jarek RL (2003) Software user's manual. EQ3/6, Version 8.0. Sandia National Laboratories—US Dept of Energy Report
- Wu X-D, Song J-M, Li X-G, Yuana H-M, Li N (2011) Behaviors of dissolved antimony in the Yangtze River estuary and its adjacent waters. *J Environ Monitor* 13:2292–2303